

Application of a TID Controller for the LFC of a Multi Area System using HGS Algorithm

Sambugari Anil Kumar

Department of EEE, Jawaharlal Nehru Technological University, Andhra Pradesh, India | Department of EEE, G. Pulla Reddy Engineering College (Autonomous), Andhra Pradesh, India
sanil.0202@gmail.com (corresponding author)

Mungara Siva Sathya Narayana

Department of EEE, G. Pulla Reddy Engineering College (Autonomous), Andhra Pradesh, India
varma.sathya@gmail.com

Kambali Jithendra Gowd

Department of EEE, JNTUA College of Engineering Ananthapuramu, Andhra Pradesh, India
indra.jithu@gmail.com

Received: 26 November 2022 | Revised: 30 January 2023, 7 March 2023, and 23 March 2023 | Accepted: 3 April 2023

Licensed under a CC-BY 4.0 license | Copyright (c) by the authors | DOI: <https://doi.org/10.48084/etasr.5502>

ABSTRACT

A Tilt Integral Derivative (TID) controller is designed in this paper for the Load Frequency Control (LFC) issue of a multi-area interconnected restructured power system. The suggested TID controller settings are fine-tuned using a novel optimization technique known as Hunger Games Search (HGS) algorithm. A multi-area interconnected power system with various generating units is used to test the performance of the proposed TID controller based on HGS. The suggested controller also takes into account system nonlinearities such as Generation Rate Constraints (GRCs) and Governor Dead Band (GDB). The superiority of HGS's optimization over a range of other significant optimization techniques, such as the grey-wolf optimization algorithm, has been confirmed. The simulation results show that the proposed TID controller based on HGS improves system frequency stability significantly under a variety of load perturbation scenarios.

Keywords-load frequency control; TID controller; DISCO participation matrix; Hunger Games Search (HGS), algorithm

I. INTRODUCTION

Voltage frequency is one of the most essential power system indicators. Frequency regulation in power systems has recently received much attention. One of the most basic current demands is maintaining a dependable and cost-effective electrical supply while presenting and spreading power as reliably and cost-effectively as possible in contemporary connected equipment. The magnetizing current will continue to rise in strength when the frequency is dropped, even if it is just a little amount. The transformer, especially its center, may get saturated as a result of the increased current flowing through it, and the coil may burn out. Maintaining a balanced electric grid is tough due to the rising demand for power. Throughout the operation of electrical equipment, weight is constantly converted. The frequency of the tool has a negative connection with the mechanical output strain of the generator [1-4]. Three layers of frequency regulation are largely unambiguous: primary, secondary, and tertiary. Before the under/over frequency protection relays are triggered, the primary frequency control loop intercepts the frequency fall. The

governor droop is commonly used for main frequency regulation, resulting in consistently reported errors. The secondary frequency control, also known as Load Frequency Control (LFC) or Automatic Generation Control (AGC), regulates the frequency in power systems with two main goals: (i) maintaining the frequency in a desirable range and (ii) controlling the interchange power through major tie lines between the different control areas. After a severe disruption, the primary responsibility of the tertiary control level is to re-dispatch generating units and auxiliary reserves. Because no interconnected system modification is required, the single-area LFC system's goal is limited to stabilizing operating frequency to the nominal value. To achieve load balance at the local and global levels in a multi-area LFC system, each area's generators must regulate the local load and tie-line power fluctuations from connecting areas. Frequency control is performed by adding the ACE signal to the feedback loop, which not only accounts for variations in frequency and power exchange, but also for the energy and time inaccuracy caused by schedule and device irregularities. Due to the deregulation of the electrical

industry, the incentives and indicators provided by the government to firms for controlling and managing their operations have shifted significantly. Electric utilities, including GENCOs, TRANSCO, and DISCOMs as part of the DISCO tool, have been liberalized as a top-tier job that is now available to anybody interested in working in the business. An Independent System Operator (ISO), which is a huge

corporation, is in charge of keeping track of open market users. In deregulated electric systems, AGC structures will almost definitely continue to be essential, yet, the operations of AGC systems in a vertically integrated agency and those in an unstructured device differ greatly in terms of some methods [5-9].

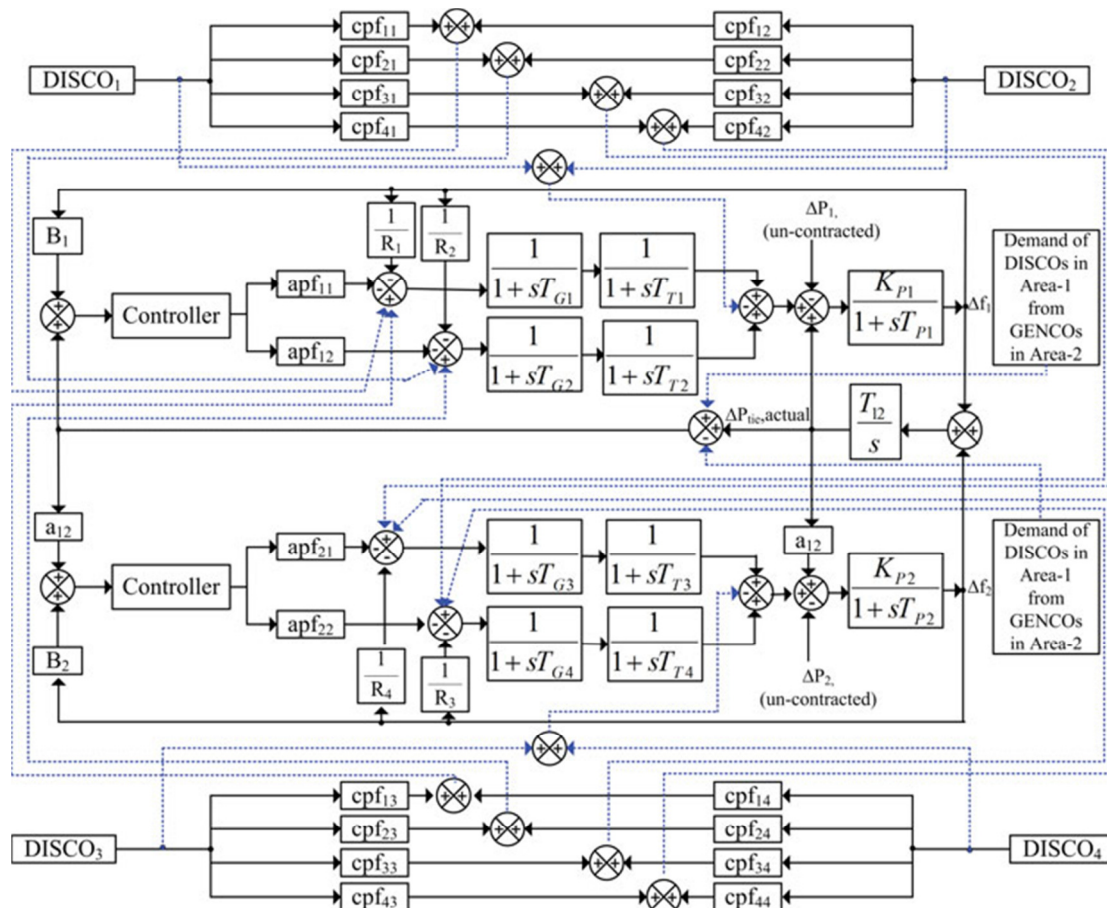


Fig. 1. Block diagram of a multi area deregulated system.

AGC systems will continue to play a crucial role in the management of out-of-control electric power networks, regardless of the outcome. AGC structures will almost certainly continue to be important in unregulated electric systems, however, the operations of AGC systems in a vertically integrated agency and those in an unstructured device differ significantly in some ways [10-16]. Based on the work of the fundamental elements of conventional algebraic geometric computation are the proportional, integrals, and derivatives, as well as their combinations. PID is the most frequently used LFC manipulation [17-18], in part because of its simplicity, dependability, and wide range of applications. Nonlinear parameters include the Governor Dead Band (GDB) and the Generation Rate Constraint (GRC) that has an impact on the performance of LFCs [19-20]. When confronted with LFC stressful events, many recent responses were supplied that allowed us to improve the dynamic behavior of the system. Different optimization techniques are evaluated in [21-27].

Many researchers were concerned about the overall performance of PID and TID controllers in the LFC when it came to evaluating the controllers' overall performance [28-30].

II. MULTI-AREA DEREGULATED SYSTEM

A. The Traditional Electric Power System Scenario

The traditional electricity market, which includes all generation, transmission, and distribution units, is consolidated under a single utility with total operational control. A single utility firm may directly supply, transmit, and distribute electricity to customers. Utility companies must follow the power charge set by each state's electrical commission. Because a single utility controls all the power, this status is known as a monopoly.

B. The Deregulated Energy System Scenario

Deregulation refers to the process of modifying the laws and regulations of the electric power industry so that customers have a choice of electricity providers. Figure 1 refers to a deregulated energy market that allows for competition among shareholders to purchase and sell electricity and invest in electric power plants and transmission lines. The shareholders of the Generation Company subsequently sell wholesale power to retail firms, who ultimately charge consumers based on the retail electricity estimated price.

C. Disco Participation Matrix

The current AGC system has two areas, each with two-generation stations, namely a thermal power generation unit, and a solar power unit. There are two types of GENCOs and DISCOMs in each area. The entire fractional amount of load dealt by DISCO from a GENCO is represented by the contract participation factor in each element. Because the GENCO must give the needed load to the DISCO regardless of the location or conditions, the sum of the components in each column equals unity in the DISCO Participation Matrix (DPM):

$$DPM = \begin{bmatrix} cpf_{11} & cpf_{12} & cpf_{13} & cpf_{14} \\ cpf_{21} & cpf_{22} & cpf_{23} & cpf_{24} \\ cpf_{31} & cpf_{32} & cpf_{33} & cpf_{34} \\ cpf_{41} & cpf_{42} & cpf_{43} & cpf_{44} \end{bmatrix}$$

III. DESIGN OF CONTROLLERS

The Tilt Integral Derivative (TID) controller is a feedback-type controller, similar to the PID controller and with the same advantages, while also having greater dynamic properties. Both controllers have identical integral and derivative actions, but the proportional action of the PID controller is replaced with a tilt-proportional controller with internal feedback which is shown in Figure 2. The objective function is given by:

$$J = \int_0^{t_{sim}} (\Delta f_i)^2 + (\Delta f_z)^2 + (\Delta P_{tie})^2 dt \quad (1)$$

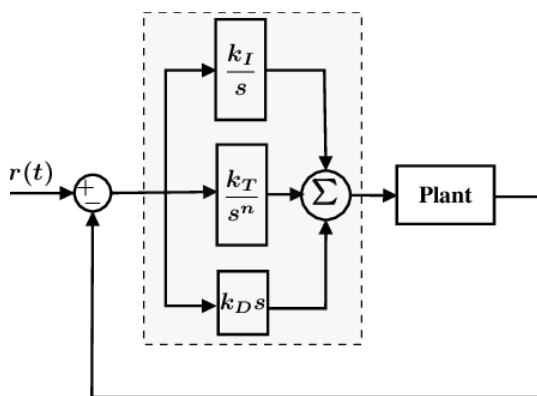


Fig. 2. TID controller block diagram.

IV. HUNGER GAMES SEARCH (HGS) ALGORITHM

HGS was proposed in 2021. The dynamic, fitness-based search technique for new users and decision-makers uses

"Hunger," an animal's fundamental homeostatic drive, as a guiding factor. HGS incorporates the concept of hunger into its feature process. An adaptive weight is built and utilized to simulate the effect of hunger on each search phase in Figure 3. It follows practically all species' computationally logical rules (games), and these competitive activities and games are frequently adaptive and evolutionary in nature, ensuring enhanced chances of survival and food acquisition. The method is more efficient than current optimization approaches due to its dynamic nature, simple structure, and outstanding performance in terms of convergence and acceptable solution quality. The convergence curve of the HGS algorithm is shown in Figure 14.

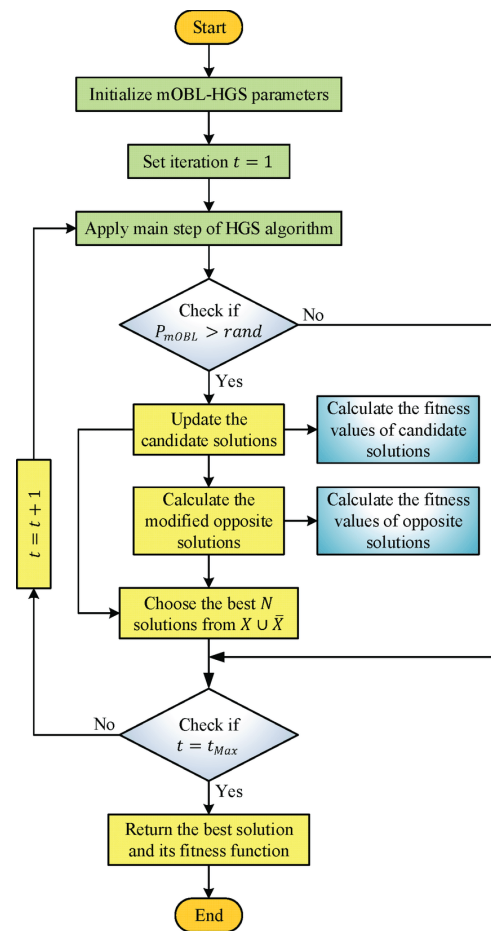


Fig. 3. Flowchart of the HGS algorithm.

1) STEP: 1 Approach Food

$$\overline{X}(t+1) = \begin{cases} \overline{X}(t) \cdot (1 + randn(1)), & r_2 < l \\ W_1 \cdot \overline{X}_b + \overline{R} \cdot W_2 \cdot |\overline{X}_b - \overline{X}(t)|, & r_1 > l, r_2 > E \\ W_1 \cdot \overline{X}_b + \overline{R} \cdot W_2, & r_1 > l, r_3 > E \end{cases} \quad (2)$$

where R is the range of $[-a, a]$, r_1 and r_2 are random numbers in the range of $[0,1]$, $randn(1)$ is a random number satisfying normal distribution, X_b is the location information of a random individual in all the optimal individuals, t is the current

iteration, W_1 and W_2 are the weights of hunger, $X(t)$ is each individual's location, and l is the parameter setting experiment.

The formula for E is:

$$E = \sec h|F(i) - BF| \tag{3}$$

where $i \in 1, 2, 3, \dots, n$, $F(i)$ is the fitness value of each individual, and BF is the best fitness value.

$$\bar{R} = 2a \times rand - a \tag{4}$$

where $a = 2 \times (1 - \frac{t}{max_iter})$, $rand$ is a random number in the range of $[0,1]$, and max_iter is the maximum number of iterations. The starvation characteristics of individuals in search are simulated mathematically.

B. STEP: 2 Hunger Role

$$\overline{W}_1(l) = \begin{cases} hungry(i) \times \frac{N \times r_4}{SHungry} & , r_3 < l \\ 1 & , r_3 \geq l \end{cases} \tag{5}$$

$$\overline{W}_2(l) = (1 - e^{-|hungry(i) - SHungry|}) \times r_5$$

where $hungry$ is the hunger of each individual, N is the number of individuals, $SHungry$ is the sum of hunger feelings of all individuals, and r_3, r_4, r_5 are random numbers ranging in $[0,1]$.

$$hungry(i) = \begin{cases} 0 & , AllFitness(i) = BF \\ hungry(i) + H & , AllFitness(i) \neq BF \end{cases} \tag{6}$$

where $AllFitness(i)$ is the fitness of each individual in the current iteration and H is acquired by:

$$TH = \frac{F(i) - BF}{WF - BF} \times r_6 \times 2 \times (UB - LB) \tag{7}$$

$$H = \begin{cases} LH \times (1 + r) & , TH < LH \\ TH & , TH \geq LH \end{cases} \tag{8}$$

V. RESULTS AND DISCUSSION

Each area consists of one solar system and one thermal system as shown in Figure 4. To evaluate the most recent TID controller, it is important to employ a deregulated electricity system. Nonlinear components, such as GRC and GDB, are assessed in addition to linear components. Steam must be able to circulate through the turbine and condense on the supplied contractions for GRC to work. Water droplets collide with turbine blades due to the presence of condensed steam, causing them to eventually stop operating. A GRC restriction of 0.05% is implemented. In the absence of torque, GDB is better characterized as the pace at which the steam valve characteristic can be swapped. When the GDB is used, a 0.06% restriction is possible.

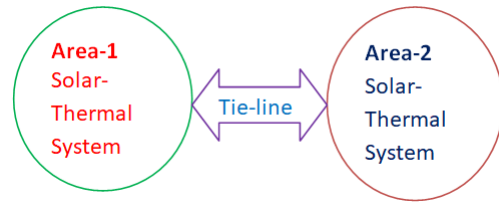


Fig. 4. The single line diagram of a two-area system.

A. Case A: Pool Co-based Transaction

A pool co-based transaction occurs when a DISCO shares a load with any of the GENCOs in the same area. The area participation factor is 0.5 when the 4 values are the same. Figures 5-7 use different HGS-based and GWO-based controllers, showing the difference in frequency in each area and the power of the tie line. Table I shows that the HGS-based controller performs better for pool co-based transactions than the GWO-based controller.

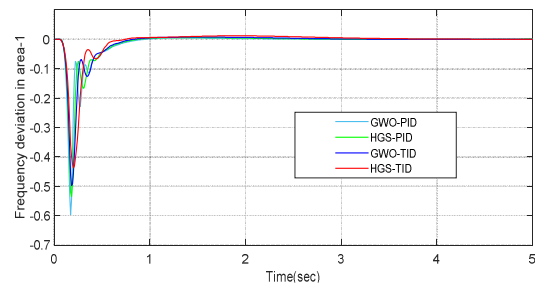


Fig. 5. Deviation of frequency in area-1 under pool co-based transaction for 1% step load disturbance.

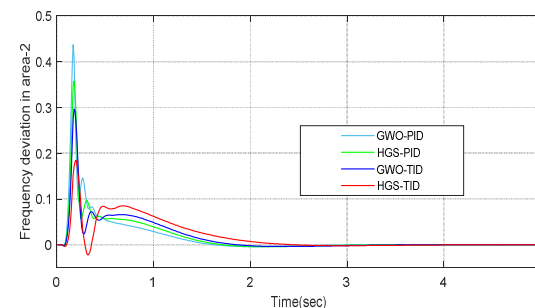


Fig. 6. Deviation of frequency in area-2 under pool co-based transaction for 1% step load disturbance.

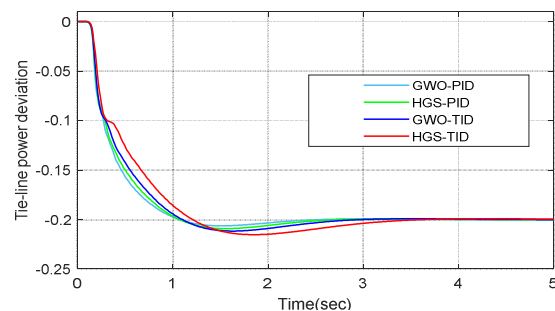


Fig. 7. Tie line energy deviation beneath a pool co-based transaction for a 1% step load disturbance.

TABLE I. COMPARISON OF OVERSHOOT, UNDERSHOOT, AND SETTLING TIME UNDER POOL CO-BASED TRANSACTIONS

	μ_p (peak overshoot)			μ_u (peak undershoot)			S.T. (settling time)		
	Δf_1	Δf_2	ΔP_{tie}	Δf_1	Δf_2	ΔP_{tie}	Δf_1	Δf_2	ΔP_{tie}
GWO-PID	-	0.42	-	0.6	-	0.22	1.8	2.5	3.4
HGS-PID	-	0.35	-	0.52	-	0.22	1.6	2.2	3.2
GWO-TID	-	-0.28	-	0.5	-	0.21	1.4	1.8	3
HGS-TID	-	-0.18	-	0.42	-	0.21	1.2	1.6	2.8

B. Case B: Bilateral-based Transaction

There is a bilateral transaction that takes place whenever a DISCO shares the load with any of the GENCOs in another region. The values that should be used for the area participation factor for the 4 values that are considered uneven are 0.75, 0.25, 0.5, and 0.5. Figures 8-10, employing various HGS-based and GWO-based controllers, respectively, depict the deviation of frequency in area-1, area-2, and tie line power. Table II demonstrates that, for bilateral-based transactions, the HGS-based controller performs better than the GWO-based controller.

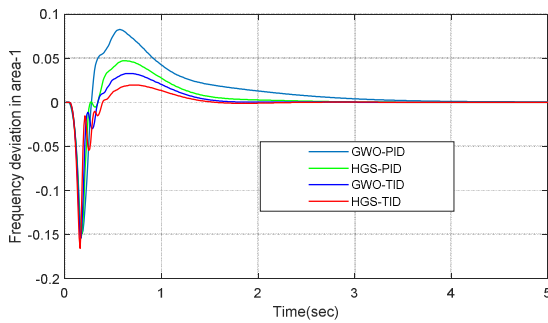


Fig. 8. Deviation of frequency in area-1 under bilateral-based transaction for 1% step load disturbance

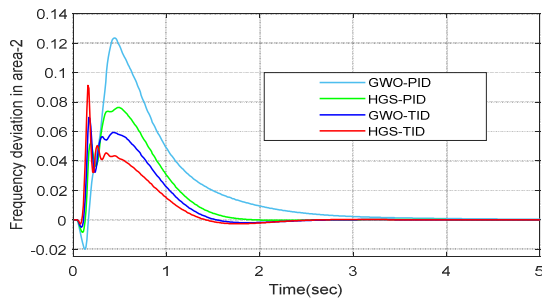


Fig. 9. Deviation of frequency in area-2 under bilateral-based transaction for 1% step load disturbance.

TABLE II. COMPARISON OF OVERSHOOT, UNDERSHOOT, AND SETTLING TIME UNDER BILATERAL-BASED TRANSACTIONS

	μ_p (peak overshoot)			μ_u (peak undershoot)			S.T. (settling time)		
	Δf_1	Δf_2	ΔP_{tie}	Δf_1	Δf_2	ΔP_{tie}	Δf_1	Δf_2	ΔP_{tie}
GWO-PID	0.08	0.12	-	0.15	-	0.05	3.2	3.6	3.2
HGS-PID	0.05	0.08	-	0.15	-	0.05	2.8	2.8	3.0
GWO-TID	0.03	0.09	-	0.15	-	0.05	2.4	2.4	2.8
HGS-TID	0.02	0.06	-	0.18	-	0.05	2.2	2.2	2.6

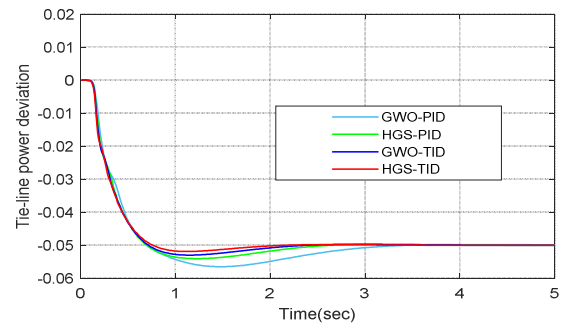


Fig. 10. Deviation of tie line power under bilateral-based transaction for 1% step load disturbance.

C. Case C: Contract Violation

When the DISCO requests more electricity than the agreed-upon value, a contract violation arises. GENCO does not lease out this extra power. A GENCO in the same vicinity as the DISCO should supply this uncontracted power. Let's consider instance 2, which necessitates adding 0.1 p.u. MW of power to a DISCO1. Figures 11-13 which use various HGS-based, and GWO-based controllers, respectively, demonstrate the deviation of frequency in area-1, area-2, and tie line power. Table III demonstrates that, in a contract violation-based transaction, an HGS-based controller performs better than GWO-based controller.

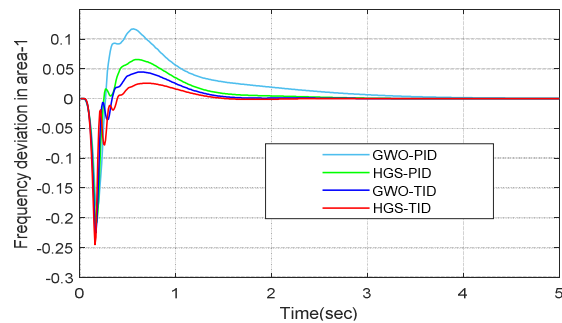


Fig. 11. Deviation of frequency in area-1 under contract violation for 1% step load disturbance.

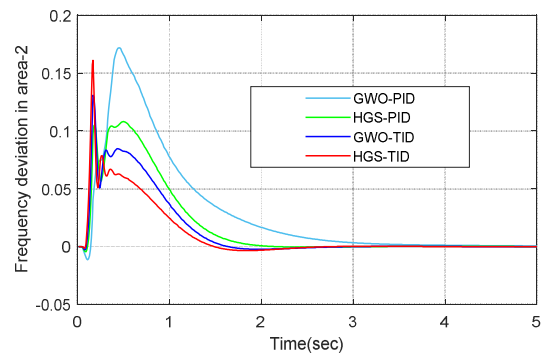


Fig. 12. Deviation of frequency in area-2 under contract violation for 1% step load disturbance.

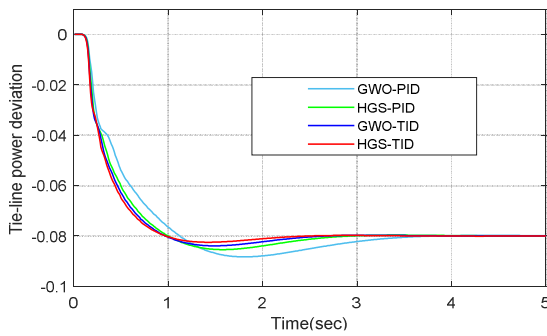


Fig. 13. Deviation of tie-line power under contract violation for 1% step load disturbance.

TABLE III. COMPARISON OF OVERSHOOT, UNDERSHOOT, AND SETTLING TIME UNDER CONTRACT VIOLATION BASED TRANSACTIONS

	μ_p (peak overshoot)			μ_u (peak undershoot)			S.T. (settling time)		
	Δf_1	Δf_2	ΔP_{tie}	Δf_1	Δf_2	ΔP_{tie}	Δf_1	Δf_2	ΔP_{tie}
GWO-PID	0.1	0.17	-	0.24	-	0.09	3.5	3.8	3.2
HGS-PID	0.05	0.16	-	0.24	-	0.09	3.2	2.4	3.0
GWO-TID	0.04	0.15	-	0.22	-	0.08	2.8	1.8	2.8
HGS-TID	0.02	0.12	-	0.22	-	0.08	2.6	1.6	2.6

Furthermore, the SLP values for the reduced inertia case system have been varied from 1 to 2%, 5%, and 10% in areas, 1 and 2. The resultant transient response is shown in Figures 15-17. The plots in frequency and tie-line error are validating the robust nature of the proposed HGS algorithm.

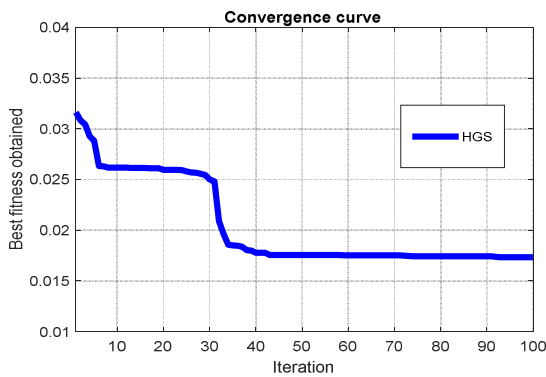


Fig. 14. Convergence curve of the HGS algorithm.

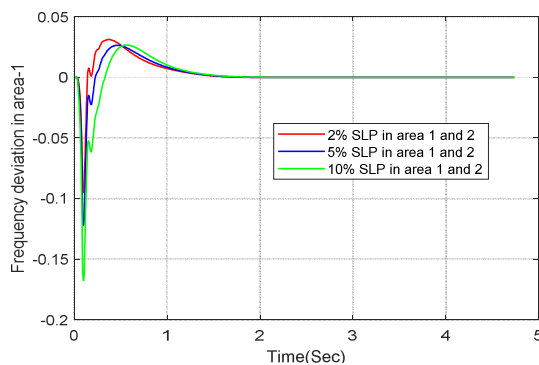


Fig. 15. Frequency deviation in area-1 for different SLP values.

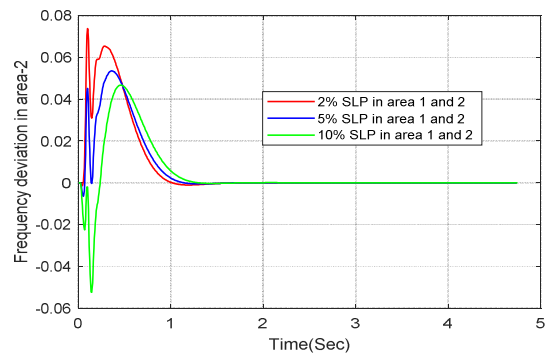


Fig. 16. Frequency deviation in area-2 for different SLP values.

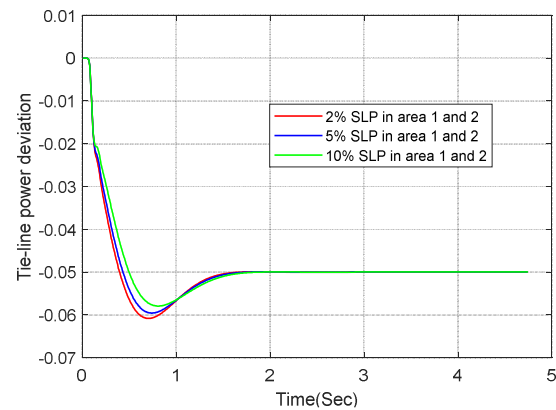


Fig. 17. Tie-line power deviation for different SLP values.

CONCLUSION

The current paper investigates the performance of a TID controller in a deregulated market structure for a variety of transactions and contract breaches. The power system's load demand is a challenging problem to handle since it necessitates the creation of several optimal controllers. The controller's major responsibility is to make sure that the voltage magnitude and frequency are always steady. The DPM strategy was put into practice. According to the comparison of the controllers, the HGS-based TID controller performs better than the GWO-based controllers in terms of settling time, overshoot, and undershoot.

APPENDIX

The system parameters are given below:

$f=50\text{Hz}$, $Tg1=0.08\text{s}$, $Tt1=0.3\text{s}$, $Tt=3\text{s}$, $Tg=1.0\text{s}$, $Tr1=10\text{s}$, $Kr1=0.5$, $Kp=120\text{Hz pu MW/rad}$, $H=5\text{s}$, $D=8.33 \times 10^{-3}\text{pu MW/Hz}$, $Tp=20\text{s}$, $T=0.086$, $Ri=2.4\text{Hz/pu MW}$, $Bi=0.425\text{pu MW/Hz}$, $Kst=1.8$, $Tst=1.8\text{s}$.

REFERENCES

[1] S. A. Kumar, M. S. S. Narayana, and K. J. Gowd, "Load frequency control of thermal system under deregulated environment using slime mould algorithm," *International Journal of Power Electronics and Drive Systems*, vol. 12, no. 4, pp. 2221–2229, 2021, <https://doi.org/10.11591/ijpeds.v12.i4>.
 [2] R. J. Abraham, D. Das, and A. Patra, "Load following in a bilateral market with local controllers," *International Journal of Electrical Power*

- & Energy Systems, vol. 33, no. 10, pp. 1648–1657, Dec. 2011, <https://doi.org/10.1016/j.ijepes.2011.06.033>.
- [3] P. Bhatt, R. Roy, and S. P. Ghoshal, "Optimized multi area AGC simulation in restructured power systems," *International Journal of Electrical Power & Energy Systems*, vol. 32, no. 4, pp. 311–322, May 2010, <https://doi.org/10.1016/j.ijepes.2009.09.002>.
- [4] H. Shayeghi and H. A. Shayanfar, "Design of decentralized robust LFC in competitive electricity environment," *Journal of Electrical Engineering*, vol. 56, no. 9–10, pp. 225–236, 2005.
- [5] Ibraheem, P. Kumar, and D. P. Kothari, "Recent philosophies of automatic generation control strategies in power systems," *IEEE Transactions on Power Systems*, vol. 20, no. 1, pp. 346–357, Oct. 2005, <https://doi.org/10.1109/TPWRS.2004.840438>.
- [6] D. V. Doan, K. Nguyen, and Q. V. Thai, "Load-Frequency Control of Three-Area Interconnected Power Systems with Renewable Energy Sources Using Novel PSO-PID-Like Fuzzy Logic Controllers," *Engineering, Technology & Applied Science Research*, vol. 12, no. 3, pp. 8597–8604, Jun. 2022, <https://doi.org/10.48084/etasr.4924>.
- [7] H. Shayeghi, H. A. Shayanfar, and A. Jalili, "Load frequency control strategies: A state-of-the-art survey for the researcher," *Energy Conversion and Management*, vol. 50, no. 2, pp. 344–353, Feb. 2009, <https://doi.org/10.1016/j.enconman.2008.09.014>.
- [8] L. C. Saikia, J. Nanda, and S. Mishra, "Performance comparison of several classical controllers in AGC for multi-area interconnected thermal system," *International Journal of Electrical Power & Energy Systems*, vol. 33, no. 3, pp. 394–401, Mar. 2011, <https://doi.org/10.1016/j.ijepes.2010.08.036>.
- [9] K. R. S. Reddy, N. P. Padhy, and R. N. Patel, "Congestion management in deregulated power system using FACTS devices," in *IEEE Power India Conference*, New Delhi, India, Apr. 2006, <https://doi.org/10.1109/POWERI.2006.1632541>.
- [10] R. C. Panda, "Synthesis of PID Tuning Rule Using the Desired Closed-Loop Response," *Industrial & Engineering Chemistry Research*, vol. 47, no. 22, pp. 8684–8692, Nov. 2008, <https://doi.org/10.1021/ie800258c>.
- [11] W. Tan, H. Zhang, and M. Yu, "Decentralized load frequency control in deregulated environments," *International Journal of Electrical Power & Energy Systems*, vol. 41, no. 1, pp. 16–26, Oct. 2012, <https://doi.org/10.1016/j.ijepes.2012.02.013>.
- [12] Y. L. Abdel-Magid and M. M. Dawoud, "Optimal AGC tuning with genetic algorithms," *Electric Power Systems Research*, vol. 38, no. 3, pp. 231–238, Sep. 1996, [https://doi.org/10.1016/S0378-7796\(96\)01091-7](https://doi.org/10.1016/S0378-7796(96)01091-7).
- [13] S. Prasad, S. Purwar, and N. Kishor, "Non-linear sliding mode load frequency control in multi-area power system," *Control Engineering Practice*, vol. 61, pp. 81–92, Apr. 2017, <https://doi.org/10.1016/j.conengprac.2017.02.001>.
- [14] S. P. Singh, T. Prakash, V. P. Singh, and M. G. Babu, "Analytic hierarchy process based automatic generation control of multi-area interconnected power system using Jaya algorithm," *Engineering Applications of Artificial Intelligence*, vol. 60, pp. 35–44, Apr. 2017, <https://doi.org/10.1016/j.engappai.2017.01.008>.
- [15] K. P. S. Parmar, S. Majhi, and D. P. Kothari, "LFC of an interconnected power system with multi-source power generation in deregulated power environment," *International Journal of Electrical Power & Energy Systems*, vol. 57, pp. 277–286, May 2014, <https://doi.org/10.1016/j.ijepes.2013.11.058>.
- [16] B. Mohanty, S. Panda, and P. K. Hota, "Controller parameters tuning of differential evolution algorithm and its application to load frequency control of multi-source power system," *International Journal of Electrical Power & Energy Systems*, vol. 54, pp. 77–85, Jan. 2014, <https://doi.org/10.1016/j.ijepes.2013.06.029>.
- [17] D. C. S. Rao, "Implementation of Load Frequency Control of Hydrothermal System under Restructured Scenario Employing Fuzzy Controlled Genetic Algorithm," *International Journal of Advanced Research in Electrical, Electronics and Instrumentation Engineering*, vol. 1, no. 1, pp. 1–6, 2012.
- [18] U. K. Rout, R. K. Sahu, and S. Panda, "Design and analysis of differential evolution algorithm based automatic generation control for interconnected power system," *Ain Shams Engineering Journal*, vol. 4, no. 3, pp. 409–421, Sep. 2013, <https://doi.org/10.1016/j.asej.2012.10.010>.
- [19] H. Haes Alhelou, M. E. Hamedani Golshan, and M. Hajiakbari Fini, "Wind Driven Optimization Algorithm Application to Load Frequency Control in Interconnected Power Systems Considering GRC and GDB Nonlinearities," *Electric Power Components and Systems*, vol. 46, no. 11–12, pp. 1223–1238, Jul. 2018, <https://doi.org/10.1080/15325008.2018.1488895>.
- [20] B. Mohanty, S. Panda, and P. K. Hota, "Differential evolution algorithm based automatic generation control for interconnected power systems with non-linearity," *Alexandria Engineering Journal*, vol. 53, no. 3, pp. 537–552, Sep. 2014, <https://doi.org/10.1016/j.aej.2014.06.006>.
- [21] N. N. Shah, A. D. Chafekar, D. N. Mehta, and A. R. Suthar, "Automatic load frequency control of two area power system with conventional and fuzzy logic control," *International Journal of Research in Engineering and Technology*, vol. 1, no. 3, pp. 343–347, Mar. 2012, <https://doi.org/10.15623/ijret.2012.0103026>.
- [22] R. K. Sahu, T. S. Gorripotu, and S. Panda, "A hybrid DE–PS algorithm for load frequency control under deregulated power system with UPFC and RFB," *Ain Shams Engineering Journal*, vol. 6, no. 3, pp. 893–911, Sep. 2015, <https://doi.org/10.1016/j.asej.2015.03.011>.
- [23] M. Ma, C. Zhang, X. Liu, and H. Chen, "Distributed Model Predictive Load Frequency Control of the Multi-Area Power System After Deregulation," *IEEE Transactions on Industrial Electronics*, vol. 64, no. 6, pp. 5129–5139, Jun. 2017, <https://doi.org/10.1109/TIE.2016.2613923>.
- [24] R. Shankar, K. Chatterjee, and R. Bhushan, "Impact of energy storage system on load frequency control for diverse sources of interconnected power system in deregulated power environment," *International Journal of Electrical Power & Energy Systems*, vol. 79, pp. 11–26, Jul. 2016, <https://doi.org/10.1016/j.ijepes.2015.12.029>.
- [25] R. K. Selvaraju and G. Somaskandan, "Impact of energy storage units on load frequency control of deregulated power systems," *Energy*, vol. 97, pp. 214–228, Feb. 2016, <https://doi.org/10.1016/j.energy.2015.12.121>.
- [26] D. V. Doan, K. Nguyen, and Q. V. Thai, "A Novel Fuzzy Logic Based Load Frequency Control for Multi-Area Interconnected Power Systems," *Engineering, Technology & Applied Science Research*, vol. 11, no. 4, pp. 7522–7529, Aug. 2021, <https://doi.org/10.48084/etasr.4320>.
- [27] S. Pahadasingh, C. Jena, C. K. Panigrahi, and B. P. Ganthia, "JAYA Algorithm-Optimized Load Frequency Control of a Four-Area Interconnected Power System Tuning Using PID Controller," *Engineering, Technology & Applied Science Research*, vol. 12, no. 3, pp. 8646–8651, Jun. 2022, <https://doi.org/10.48084/etasr.4891>.
- [28] S. A. Kumar, M. S. S. Narayana, and K. J. Gowd, "Application of TID controller in LFC of two area system under open market scenario," in *2nd International Conference on IoT Based Control Networks and Intelligent Systems*, Kerala, India, Jun. 2021, pp. 1–11.
- [29] S. A. Kumar, M. S. S. Narayana, and K. J. Gowd, "Two area LFC of thermal system under open market scenario using Hunger Games Search Algorithm," *International Journal of Special Education*, vol. 37, no. 3, pp. 4098–4109, 2022.
- [30] S. A. Kumar, M. S. S. N. Varma, and K. J. Gowd, "Load frequency control of multi area system under deregulated environment using artificial gorilla troops optimization," *Bulletin of Electrical Engineering and Informatics*, vol. 11, no. 6, pp. 3051–3060, Dec. 2022, <https://doi.org/10.11591/eei.v11i6.4188>.